Robust coordinated rendezvous of depth-actuated drifters in ocean internal waves

M. Ouimet [a] J. Cortés [a]

[a] *Department of Mechanical and Aerospace Engineering, University of California, San Diego, CA, 92093, USA*

Abstract

This paper considers a team of spatially distributed drifters that move underwater under the influence of an ocean internal wave. The overall objective is for the drifters to use the known depth-dependent ocean flowfield to rendezvous underwater and then return to the surface as a cluster for easy retrieval. From the structure of the internal wave, the ocean flowfield is time-varying and spatially dependent on depth and position along the wave propagation direction. The drifters can control their depth by changing their buoyancy and are otherwise subject to the horizontal flowfield at their given depth. We consider two different drifter dynamical models: a first-order Lagrangian model, useful when the drifter's mass is sufficiently small, and a second-order linear model, where the drag force caused by the water accelerates the drifter. We design provably correct distributed algorithms that rely on the drifters opportunistically changing their depth so that the ocean flowfield takes them in a desirable direction to perform coordinated motion. Under the proposed algorithms, the drifters converge asymptotically to the same depth and position along the wave propagation direction. We also investigate the algorithms' robustness against errors in actuation, estimation of the wave parameters, or state measurements. Various simulations illustrate our results.

Key words: oceanic drifters, internal waves, coordinated rendezvous, collective motion

1 Introduction

Internal waves are waves that propagate within a fluid, rather than on its surface. They are of particular interest to marine ecologists and oceanographers because they are agents of transport for planktonic organisms, larvae, and small fish. The type considered here arise when deep oceanic water is disturbed. Normally, water density varies continuously with depth and surfaces of constant density are at a fixed depth. However, when the water receives an energetic disturbance, it leads to time-varying, sinusoidal profiles in the surfaces of constant density. This, in turn, gives rise to a nonlinear, depth- and time-varying dynamical model for the ocean, which can be parameterized by constants such as amplitude, wavenumber, and frequency. In these scenarios, one can envision using a team of robotic drifters to perform the dual task of estimating the parameters that define the ocean flowfield induced by the internal wave and then using this knowledge to perform motion control. Here we are interested in distributed control algorithms for rendezvous. Our focus is motivated by practical considerations of easy recovery: when oceanographers deploy these robotic sensors, they must retrieve them after the data is collected. However, with long deployment times, the drifters may drift miles apart. For large numbers of robots, this recovery task becomes time-consuming. Active control is also useful for recovering drifters measuring water properties underneath ice caps. In this more challenging problem, drifters must rendezvous as well as reach the ice hole they were dropped in for recovery. The rendezvous problem, however, is challenging because the drifters can only control their depth by changing their buoyancy and are otherwise subject to the horizontal flowfield of the ocean at their given depth. The basic idea of our strategy is for drifters to opportunistically change their depth so that the ocean flowfield takes them in a desirable direction to perform coordinated motion.

Literature review: Internal waves are associated with high concentrations of various types of planktonic organisms and small fishes [Zeldis and Jillett, 1982, Shanks, 1983], as well as an agent of larval transport [Pineda, 1999]. This makes their study important to oceanographers, see e.g. [Lennert-Cody and Franks, 1999, Susanto et al., 2005] and references therein. Many internal wave models exist in the literature [Osborne and Burch, 1980, Hamdi et al., 2011]; here, we consider a continu-

⋆ A preliminary version of this paper appeared as [Ouimet and Cortés, 2014a] at the 2014 IEEE Conference on Decision and Control.

Email addresses: miouimet@ucsd.edu (M. Ouimet), cortes@ucsd.edu (J. Cortés).

ously depth-dependent model found in [Thorpe, 1968]. Scientists widely use drifters drifting passively as monitoring platforms to gather relevant ocean data [Perry and Rudnick, 2003, Freeland and Cummins, 2005, Han et al., 2010]. The use of autonomous underwater vehicles to detect and characterize internal waves is a relatively new approach. Whereas previous works use ocean measurements such as conductivity, temperature, pressure data [Cazenave, 2008, Petillo and Schmidt, 2013] or vertical flow velocity [Zhang et al., 2001] to detect and analyze internal waves, our recent work [Ouimet and Cortés, 2014b] is unique in using inter-vehicles measurements for depth-independent internal wave models. This work is also connected to the increasing literature that deals with cooperative networks of agents estimating spatial natural phenomena, including ocean [Leonard et al., 2007, Paley et al., 2008, Graham and Cortés, 2012], river [Ru and Martínez, 2013], and hurricane sampling [DeVries and Paley, 2012]. Furthermore, it is tied to works related to motion planning in oceanic flows. Recent work [Jouffroy et al., 2013] explores the possibility of actively utilizing tidal currents so that drifters can autonomously reach a desired destination. The flowfield considered there is a time-varying model with no horizontal spatial dependency and a piecewise-constant dependency on depth. This simplicity allows the drifter to achieve its objective by only sensing which way the current is going, its depth, and the relative distance between itself and the goal location. Other researchers have also dealt with marine robots moving through strong flowfields where their actuation is limited and therefore cannot completely compensate the flow [Paley and Peterson, 2009, Kwok and Martínez, 2012]. Because the drifters control their vertical velocity which, in turn, affects their depth-dependent horizontal velocity, we adopt a backstepping framework [Khalil, 2002] where we first design a controller based on Laplacian agreement dynamics [Ren and Beard, 2008] assuming direct control and then we design the depth-controller for the full system.

Statement of contributions: We consider a group of robotic drifters that seek to coordinately rendezvous underwater while moving in an ocean flowfield induced by a depth-dependent internal wave. Our starting point is the assumption that the parameters that determine the internal wave are known to the drifters. We develop distributed cooperative strategies that allow the drifters to asymptotically rendezvous under two different dynamical models. In the first (Lagrangian) model, we assume that the drifters are sufficiently small so that their velocity is equal to that of the ocean's velocity at their current location. In the second (drag-based) model, we assume that drifters are accelerated by a drag force proportional to the difference in their velocity and the ocean's. The coordinated rendezvous problem is challenging because of two reasons. First, since the drifters may only directly change their vertical depth in the water column, they must rely on the horizontal current at their current depth to move them towards rendezvous. Second, the flowfields are time-varying, creating situations where periodically the drifters have not enough (or even completely lack) control authority. Our technical approach is divided into two stages. First, assuming drifters have direct control in the horizontal direction, we design a provably correct law, that we term 'virtual', that allows all drifters to rendezvous despite the time-varying control authority. Second, we design a depth-control law for the true system and establish its convergence to the virtual control law in finite time, from which we deduce the desired asymptotic rendezvous property for the full dynamics. We also investigate the robustness properties of the proposed algorithms against errors in actuation and in the knowledge of the flowfield or the state of other drifters. We provide a bound on the maximum error size in the depth-control law with which the drifters still rendezvous. When the virtual control law is corrupted by additive errors, we show that the drifters converge to a neighborhood around each other. Various simulations illustrate our results.

Organization: Section 2 contains notation and preliminaries and Section 3 contains the wave and drifter models along with our problem statement. Section 4 contains the proposed algorithm, the proof of its correctness, and its robustness properties for a first-order drifter model and Section 5 contains the proposed algorithm and the proof of correctness for a second-order drifter model. Finally, Section 6 contains our conclusions and some directions of future work.

2 Preliminaries

This section introduces basic notation and preliminaries used throughout the paper.

2.1 Notation

Let $\mathbb{R}$, $\mathbb{R}_{\geq 0}$, and $\mathbb{R}_{>0}$ denote the set of real, nonnegative real, and positive real numbers, respectively. We use $\mathbf{1}_d$ and $\mathbf{0}_d \in \mathbb{R}^d$ to denote the vectors of all ones and all zeros, respectively. We use $\|\cdot\|_2$ to denote the Euclidean norm. For a finite set P, $\mathrm{card}(P)$ denotes its cardinality. Given $M \in \mathbb{R}_{>0}$, the saturation function $\mathrm{sat}_M : \mathbb{R} \times \mathbb{R}_{>0} \to \mathbb{R}$ is defined as

$$\mathrm{sat}_M(x) = \begin{cases} M, & x > M, \\ x, & -M \leq x \leq M, \\ -M, & x < -M. \end{cases}$$

The sign function $\mathrm{sgn} : \mathbb{R} \to \mathbb{R}$ is defined as

$$\mathrm{sgn}(x) = \begin{cases} 1, & x > 0, \\ 0, & x = 0, \\ -1, & x < 0. \end{cases}$$

Given $x \in \mathbb{R}^d$, we let $x_{\min}$, respectively $x_{\max}$, be the smallest, respectively largest, component of x.

2.2 Graph theory

We discuss here some basic graph theory following the exposition in [Bullo et al., 2009]. Let $G = (V, E)$ be an

undirected graph with N vertices $V = \{1, \ldots, N\}$ and edges $E \subseteq V \times V$. A path in graph G is an ordered sequence of vertices such that any pair of consecutive vertices in the sequence is an edge of the graph. A graph is connected if there exists a path between any two vertices. The neighbor set of vertex $v \in V$ is the set of vertices it has edges to, $\mathcal{N}_v = \{v' \in V \backslash \{v\} \mid (v, v') \in E\}$. The Laplacian matrix $L(G) = (\ell_{i,j})_{n \times n}$ associated with G is defined by,

$$\ell_{i,j} = \begin{cases} \text{card}(\mathcal{N}_i), & \text{if } i = j, \\ -1, & \text{if } i \neq j \text{ and } (i,j) \in E, \\ 0, & \text{otherwise.} \end{cases}$$

Note that $L(G)\mathbf{1}_n = \mathbf{0}_n$. This matrix is symmetric and positive semidefinite, with the multiplicity of 0 corresponding to the number of connected components of G. For connected graphs, the following inequality, taken from [Nowzari and Cortés, 2014], will be useful later

$$\lambda_2(L) x^T L x \leq x^T L^2 x \leq \lambda_n(L) x^T L x, \tag{1}$$

where $\lambda_2(L)$ and $\lambda_n(L)$ denote the smallest non-zero and largest eigenvalue of L, respectively.

2.3 Stability analysis

Here, we recall some useful results that are later employed in our technical approach. We begin with Barbalat's Lemma, which characterizes the asymptotic behavior of a certain class of functions.

Lemma 2.1 (Barbalat's Lemma [Khalil, 2002]) *Let $\phi : \mathbb{R}_{\geq 0} \to \mathbb{R}$ be a uniformly continuous function. Suppose that $\lim_{t \to \infty} \int_0^t \phi(\tau) d\tau$ exists and is finite. Then, $\phi(t) \to 0$ as $t \to \infty$.*

This result is particularly useful when analyzing the asymptotic behavior of trajectories of time-dependent dynamical systems, as the ones considered in this paper.

3 Problem statement

This section presents the internal wave and depth-actuated drifter models, and then provides a formal problem statement.

3.1 Internal wave model

We specify the internal wave model in a global reference frame $\Sigma = (\mathbf{p}, \{\mathbf{e}_x, \mathbf{e}_y, \mathbf{e}_z\})$, defined as follows. The origin $\mathbf{p}$ is an arbitrary point at the ocean surface; the vector $\mathbf{e}_x$ corresponds to the direction of wave propagation, which we assume parallel to the ocean bottom, and $\mathbf{e}_z$ is perpendicular to the ocean bottom, pointing from bottom to surface. The coordinates induced by Σ are denoted by $\{x, y, z\}$.

Following [Thorpe, 1968], we consider a continuously stratified density profile and the mode-1 internal waves produced in it. Here, a fluid has a finite depth H and the density increases linearly from ocean surface to ocean bottom. This leads to the following horizontal and vertical flowfields, respectively, induced by the presence of the internal wave,

$$f_x(x, z, t) = \frac{\alpha \pi}{H} \cos\left(\frac{\pi z}{H}\right) \sin(kx - \omega t + \phi), \tag{2a}$$

$$f_z(x, z, t) = -\alpha k \sin\left(\frac{\pi z}{H}\right) \cos(kx - \omega t + \phi). \tag{2b}$$

Here, α is the ordering parameter proportional to the wave amplitude, k is the horizontal wavenumber, ω is the frequency, and ϕ is the initial condition for phase. The flowfield can be seen in Figure 1.

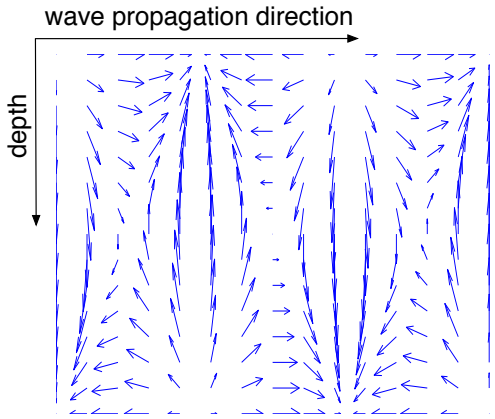

Fig. 1. The plot illustrates the dependency of internal wave flowfield cf. (2) as a function of depth (-z-direction) and wave propagation direction (+x-direction) at one time instant. As the wave propagates to the right, the flowfield translates to the right at a fixed speed.

In the ocean, it is not always a valid assumption that an internal wave exists in isolation of other phenomena such as tides. However, a time-varying addition to the flowfield which is spatially constant over the drifters' spatial scale affects all drifters equally. With a change of coordinates, these types of additive currents can be removed, making our simplified oceanic flowfield applicable.

Note that this wave model does not produce motion in the y-direction and it depends continuously on depth as a result of the dependency of density on depth. This adds an additional layer of complexity and realism with respect to simpler, two-layer fluid models where the flowfield changes discontinuously at the wave interface, such as the ones considered in [Franks, 1997, Lennert-Cody and Franks, 1999]. In fact, our developments in this paper are based on the observation that the added complexity from depth-dependent flowfields can be leveraged to allow for coordinated motion of the drifters, as we explain in the problem statement below. We finish this section by noting that there exist other continuously stratified models for internal waves, see [Thorpe, 1968], such as the hyperbolic tangent model capturing the density depth profile of deep ocean water. Although we do not consider them for reasons of space, our proposed design could be adapted to produce similar results to the

ones presented here. In general, little is known about the ocean flowfields at small temporal and spatial scales (such as the specific models for internal waves), providing a motivating purpose for researchers to use drifters to estimate them.

3.2 Drifter model

A drifter is a submersible buoy which can drift in the ocean, unattached to the ocean floor or a boat, and is able to change its vertical velocity in the water by controlling its buoyancy. We assume a drifter can measure its own absolute position and the position of nearby drifters. Even though GPS is not available underwater, oceanographers have other means to achieve this in areas of limited size by deploying a grid of acoustic near-surface pingers, for instance. The drifters, equipped with hydrophones, can determine their location based on the travel time of the pingers' pulses [Jaffe Laboratory for Underwater Imaging, 2014, Techy et al., 2010]. Given a drifter's absolute position information, either relative or absolute position information about neighboring drifters can be used to infer absolute position information. This could be from a sensing instrument like sonar or via communication using acoustic modems over relatively short ranges (and utilizing stationary relays/amplifiers for a longer range). In the presented algorithm, drifters also require velocity and acceleration measurements, which we assume can be estimated by numerical differentiating the position signals. Our colleagues at Scripps Institute of Oceanography [Jaffe Laboratory for Underwater Imaging, 2014] have an autonomous underwater vehicle team that can localize from acoustic pingers. Although their current prototype does not have a method to get position information of neighboring vehicles, they are currently working on a version that is able to communicate using acoustic modems.

Consider a group of N drifters, each with a reference frame $\Sigma_i = (\mathbf{p}_i, \{\mathbf{e}_{x_i}, \mathbf{e}_{y_i}, \mathbf{e}_{z_i}\}), i \in \{1, \dots, N\}$, attached to it. The origin $\mathbf{p}_i$ corresponds to the location of the drifter. In general, this reference frame might not be aligned with the global wave frame Σ. However, we assume that the drifters know the rotation between frames. This assumption is for simplicity of exposition. For instance, our previous work [Ouimet and Cortés, 2014b] shows how each drifter can determine the rotation between its local frame and the global frame by using relative distance and distance derivative measurements.

Different models exist to describe an object's dynamics within an ocean flowfield. The most widely used is a first-order Lagrangian dynamics, where the drifter's velocity is equal to ocean's velocity at its current location,

$$\dot{x}_i = f_x(x_i, z_i, t), \tag{3a}$$
$$\dot{z}_i = f_z(x_i, z_i, t) + u_i. \tag{3b}$$

Dropping the Lagrangian assumption, one can consider a second-order dynamics where the object is accelerated by a force governed by Stokes drag,

$$\dot{x}_i = v_i, \tag{4a}$$
$$\dot{v}_i = -\frac{c_d}{m}(v_i - f_x(x_i, z_i, t)) \tag{4b}$$
$$\dot{z}_i = f_z(x_i, z_i, t) + u_i. \tag{4c}$$

This model is suitable for objects that are in laminar flows or are very small. Note that as the mass m tends to zero, the second-order dynamics model becomes the first-order Lagrangian model. We develop algorithms for both drifter dynamic models above. In both cases, we assume that the drifters' control authority u_i is capable of counteracting the vertical velocity. In addition, there is a finite amount of available control authority M remaining. Thus, with a slight abuse of notation, we assume that the depth dynamics for each drifter i are $\dot{z}_i = u_i$, where $|u_i| \leq M$.

3.3 Problem statement

Consider a group of N spatially distributed drifters that move underwater under the influence of an ocean internal wave. Our starting point is the assumption that the drifters have determined the physical parameters that govern the motion of the internal wave. This assumption is motivated by our previous research that develops coordination algorithms for the collective estimation of such parameters. The overall objective is for the drifters to use the known ocean dynamics to rendezvous underwater and return to the surface as a cluster for easy retrieval. Formally, let the N drifters be at initial states $x(0), v(0), z(0)$. Each drifter $i \in \{1, \dots, N\}$ has access to their own state as well as its neighbors $\mathcal{N}_i$ (via either communication or sensing). We assume that the graph G induced by this exchange of state information is connected and fixed. Thus, drifter i in $\{1, \dots, N\}$ has continuous access to x_j, v_j, $\dot{v}_j$, and z_j, for j in $\mathcal{N}_i \cup \{i\}$. One possible neighbor choice is for each drifter to use the state of the drifter initially directly ahead of itself and initially directly behind itself in the wave propagation direction, i.e., a line graph.

Our objective is to design a distributed feedback coordination law that makes all drifters rendezvous at a common location in the wave propagation direction, i.e.,

$$\lim_{t \to \infty} x_i(t) - x_j(t) = 0, \qquad \forall i, j \in \{1, \dots, N\}.$$

In practical implementations, once rendezvous is achieved to a desired level of accuracy, drifters can surface synchronously near each other for easy retrieval.

4 Rendezvous of first-order drifters

This section presents our algorithmic solution for rendezvous of a group of first-order drifters. We assume that all drifters know the wave parameters, e.g., by running first the procedure in [Ouimet and Cortés, 2014b]. Since the drifters do not have direct control in the x-direction, we split the design in two steps, as described next,

[Informal description of strategy]: We employ a two-part, backstepping strategy. First, we assume that drifters can directly control their motion in the x-direction and we design a virtual control law that allows them to rendezvous. Second, we consider the true dynamics, where the control is only exerted on the drifter's depth, and design a control law that tracks the virtual control law and converges to it in finite time.

4.1 Virtual rendezvous control law

Following the outline presented above, here we design a control law that achieves rendezvous when direct control authority is available in the x-direction. Consequently, for each $i \in \{1, \dots, N\}$, we consider the dynamics

$$\dot{x}_i = \frac{\alpha\pi}{H} w_i \sin(kx_i - \omega t + \phi), \tag{5}$$

where w_i is the 'virtual' control. Specifically, we design the distributed controller,

$$w_i(x,t) = -A \tanh(Lx)_i \sin(kx_i - \omega t + \phi), \tag{6}$$

where $A \in \mathbb{R}_{>0}$ is a design parameter, so that the closed-loop dynamics is

$$\dot{x}_i = -A \frac{\alpha\pi}{H} \tanh(Lx)_i \sin^2(kx_i - \omega t + \phi). \tag{7}$$

This controller has two terms to discuss here. The first, $-A\tanh(Lx)_i$, pushes agents in the direction of the average of their neighbors. Note that this term could be implemented with relative distance measurements. The second, $\sin(kx_i - \omega t + \phi)$, ensures that the ocean flow always pushes agents in the correct direction, as seen in (7). This second term requires absolute position information to know which direction the wave is currently going, i.e., the sign of $\sin(kx_i - \omega t + \phi)$. For instance, if one employed an acoustic Doppler current profiler (ADCP) and inertial measurement unit (IMU) to estimate water velocity as a function of depth, then one could design a controller that requires only relative positions.

The next result shows that the state of the drifters following (7) remains bounded.

Lemma 4.1 (Boundedness of the trajectories) *Given any initial condition $x(0) \in \mathbb{R}^N$ for the group of drifters, the network trajectory under (7) satisfies $x(t) \in [x(0)_{\min}, x(0)_{\max}]^N$ for all $t \geq 0$.*

PROOF. Note that to establish the invariance of the set $[x(0)_{\min}, x(0)_{\max}]^N$, it suffices to look at the dynamics (7) on its boundary. Given $x \in \text{bndry}([x(0)_{\min}, x(0)_{\max}]^N)$, consider the case when $i \in \{1, \dots, N\}$ is such that $x_i = x(0)_{\min}$. In such case, we have $\tanh(Lx)_i \leq 0$, and therefore $\dot{x}_i \geq 0$. Similarly, for the case when $i \in \{1, \dots, N\}$ is such that $x_i = x(0)_{\max}$, we have $\tanh(Lx)_i \geq 0$, and hence $\dot{x}_i \leq 0$. Therefore, the vector field (7) points towards the set $[x(0)_{\min}, x(0)_{\max}]^N$ on its boundary, and the result follows. □

We combine the boundedness of the drifters' evolution stated in Lemma 4.1 with Barbalat's Lemma, cf. Lemma 2.1, to deduce that the closed-loop dynamics (6) makes the drifters asymptotically rendezvous in the wave propagation direction.

Proposition 4.2 (Asymptotic network rendezvous) *Given any initial condition $x(0) \in \mathbb{R}^N$ for the group of drifters, the dynamics (7) makes the network rendezvous in the x-direction,*

$$\lim_{t\to\infty} x_i(t) - x_j(t) = 0, \quad \forall i, j \in \{1, \dots, N\}.$$

PROOF. Consider the disagreement function $V(x) = \frac{1}{2} x^T L x$, whose Lie derivative along (7) is

$$\mathcal{L}_{(7)} V(x(t)) = -A \frac{\alpha\pi}{H} \sum_{i=1}^{N} (Lx(t))_i \cdot \tanh(Lx(t))_i \sin^2(kx_i(t) - \omega t + \phi) \leq 0. \tag{8}$$

Since V is non-increasing and lower bounded by 0, $V(x(t))$ converges as $t \to \infty$. Therefore,

$$\lim_{t\to\infty} V(x(t)) - V(x(0)) = \lim_{t\to\infty} \int_0^t \mathcal{L}_{(7)} V(x(s)) ds,$$

exists and is finite. Furthermore, because x remains in $[x(0)_{\min}, x(0)_{\max}]^N$ by Lemma 4.1, $\frac{d}{dt}\mathcal{L}_{(7)}V(x(t))$ is bounded for all t, which implies that $\mathcal{L}_{(7)}V(x(t))$ is uniformly continuous on $\mathbb{R}_{\geq 0}$. Therefore, the application of Lemma 2.1 to $\mathcal{L}_{(7)}V(x(t))$ yields $\lim_{t\to\infty} \mathcal{L}_{(7)}V(x(t)) = 0$. Since each summand of (8) is non-positive, in the limit, all summands must converge to zero. Considering the first summand, we suppose that $\lim_{t\to\infty} \sin^2(kx_1 - \omega t + \phi) = 0$ and show a contradiction. This condition implies that $kx_1 - \omega t + \phi$ converges to the discrete set $\{\dots, -2\pi, -\pi, 0, \pi, 2\pi, \dots\}$. However, convergence to a discrete set implies convergence to one of its points, which, in turn, implies that $\lim_{t\to\infty} kx_1 - \omega t = C$, for some $C \in \mathbb{R}$, which implies that x_1 diverges as time goes to infinity, contradicting Lemma 4.1. Reasoning in a similar way, one deduces that $L(x(t))$ converges to 0 or, in other words, all drifters agree on their x-variables. □

4.2 Backstepping depth-control law

Here, we build on the developments of Section 4.1 to design a depth-control law that achieves the desired network objective for the true drifter dynamics (3). As mentioned in Section 3, we make the assumption that each drifter has enough control authority in the vertical direction to cancel the vertical motion induced by the wave, and that the magnitude of the remaining control is

bounded by M. For simplicity of presentation, we abuse notation to re-define u_i to be the control after canceling the vertical motion f_z. Thus, for each $i \in \{1, \dots, N\}$, we rewrite (3) as

$$\dot{x}_i = \frac{\alpha\pi}{H} \cos\Big(\frac{\pi z_i}{H}\Big) \sin(kx_i - \omega t + \phi), \qquad \dot{z}_i = u_i,$$

where $|u_i| \leq M$. Defining $d_i = \cos(\frac{\pi z_i}{H})$, we can rewrite the dynamics as

$$\dot{x}_i = \frac{\alpha\pi}{H} d_i \sin(kx_i - \omega t + \phi), \quad \dot{d}_i = -\frac{\pi}{H}\sqrt{1-d_i^2}\, u_i,$$

where d_i is constrained to $[-1, 1]$. We refer to it as the 'transformed depth'. Given the discussion of Section 4.1, our basic idea is to synthesize a design that makes the drifter's transformed depth track the virtual control law (6). Consequently, we define the error variables $e_i = d_i - w_i$ and rewrite the dynamics in terms of x_i and e_i as

$$\dot{x}_i = \frac{\alpha\pi}{H}\big(w_i \sin(kx_i - \omega t + \phi) + e_i \sin(kx_i - \omega t + \phi)\big), \quad \text{(9a)}$$

$$\dot{e}_i = -\frac{\pi}{H}\sqrt{1-d_i^2}\, u_i - \dot{w}_i. \quad \text{(9b)}$$

Our proposed design is the depth-control law,

$$u_i(d, x, t) = \quad (10)$$
$$\operatorname{sat}_M\Big(\frac{H}{\pi\sqrt{1-d_i^2}}(C \operatorname{sgn}(d_i - w_i(x,t)) - \dot{w}_i(x(t),t))\Big),$$

where $\dot{w}_i(x(t), t)$ is the total derivative and $C \in \mathbb{R}_{>0}$ is a design parameter. The next result shows that this controller makes the transformed depth converge to a generic virtual control law in finite time if the magnitude of the control law and its time derivative are small enough to account for the limited depth-control authority M and the design parameter C is properly chosen.

Lemma 4.3 (Finite-time convergence to virtual control law) *Let $M \in \mathbb{R}_{>0}$ and $d(0) \in (-1, 1)^N$. Suppose there exist $\epsilon, \beta \in \mathbb{R}_{>0}$ and a continuous and increasing function $h : \mathbb{R}_{\geq 0} \to \mathbb{R}_{\geq 0}$ with $h(0) = 0$ such that for an arbitrary virtual rendezvous control w_i, its magnitude and its derivative are uniformly bounded by β and $h(\beta)$, respectively, and*

$$\frac{H h(\beta)(1+\epsilon)}{\pi(1-(1+\epsilon)^2\beta^2)} \leq M. \quad (11)$$

Then, for any $C \geq h(\beta)(1+\epsilon)$, the error variables e_i, for all $i \in \{1, \dots, N\}$, evolving the dynamics (9b) *with control law* (10) *converges to* 0 *in finite time.*

PROOF. We first show that for any initial $d(0) \in (-1, 1)^N$, each d_i converges in finite time to an invariant set where u_i in (10) is not saturated. Given any i in $\{1, \dots, N\}$, note that $\dot{d}_i < 0$ for $d_i > \beta$ and $\dot{d}_i > 0$ for $d_i < -\beta$, which makes $[-\beta(1+\epsilon), \beta(1+\epsilon)]$ an invariant set for d_i. Furthermore, because of (11), u_i is unsaturated when $d_i \in [-\beta(1+\epsilon), \beta(1+\epsilon)]$ as well. On the other hand, if $|d_i(0)| \notin [-\beta, \beta]$, then

$$\dot{d}_i \leq -\min\{\frac{\pi}{H}\sqrt{1-d_i^2}M, C\}, \quad \text{if } d_i > \beta,$$
$$\dot{d}_i \geq \min\{\frac{\pi}{H}\sqrt{1-d_i^2}M, C\}, \quad \text{if } d_i < -\beta,$$

which shows that d_i converges to the invariant set in finite time. Once in this set, and given that u_i is unsaturated on it, the e_i dynamics reduces to $\dot{e}_i = -C \operatorname{sgn}(e_i)$, which converges in finite time because the initial condition satisfies $|e_i(0)| \leq 1 + \beta$. □

Because the result does not consider the exact form of the virtual control law, we are able to re-use later the designed depth-control law for second-order drifters in Section 5. The next result states that under the true dynamics (9) with distributed control among agents given by (6) and (10), all drifters rendezvous in the x-direction.

Theorem 4.4 (Asymptotic network rendezvous) *For any initial position $x(0) \in \mathbb{R}^N$, depth $z(0) \in (0, H)^N$, $\epsilon \in \mathbb{R}_{>0}$, and bound $M \in \mathbb{R}_{>0}$ on the magnitude of depth control actuation, let the magnitude A of the virtual control law* (6) *satisfy*

$$\frac{H((2|\mathcal{N}|_{\max} + k)\frac{\alpha\pi}{H}A^2 + \omega A)(1+\epsilon)}{\pi(1-(1+\epsilon)^2A^2)} \leq M,$$

and the gain $C \geq ((2|\mathcal{N}|_{\max} + k)\frac{\alpha\pi}{H}A^2 + \omega A)(1+\epsilon)$ in the depth-control law (10)*. Then, all drifters asymptotically rendezvous under the dynamics* (9) *with the controllers* (6) *and* (10)*, i.e., for all $i, j \in \{1, \dots, N\}$,*

$$\lim_{t\to\infty} x_i(t) - x_j(t) = 0, \quad \lim_{t\to\infty} z_i(t) = \frac{-H}{2}.$$

PROOF. Under the stated hypotheses, note that, for each $i \in \{1, \dots, N\}$, we have $|w_i| \leq A$ and $|\dot{w}_i(x(t), t)| \leq (2|\mathcal{N}|_{\max} + k)\frac{\alpha\pi}{H}A^2 + \omega A = h(A)$. Then, Lemma 4.3 implies that the depth-control law converges to the virtual rendezvous control law in finite time. After this, Proposition 4.2 guarantees asymptotic rendezvous in the wave propagation direction. Depth convergence follows by noting that, in finite time, $d_i(t) = w_i(t)$ and $w_i(t)$ converges to 0. □

The assumptions on A and C in Theorem 4.4 guarantee that the control law does not exert more control authority than the maximum allowed of M. They also enforce that the virtual control law never commands beyond what the ocean's velocity field can provide. Interestingly, the algorithm could be readily extended, with similar

convergence guarantees as in Theorem 4.4, to (i) switching topologies, as long as the associated graph remains connected, and (ii) directed information topologies.

Remark 4.5 (Point-to-point reconfiguration) The coordinated control law (6) allows the drifters to all rendezvous in a situation where an a priori rendezvous location is unknown. However, by considering a goal location as the sole 'virtual' robotic neighbor with no dynamics, the control law would cause each drifter to move there. Thus, the control law is also applicable in situations where a common rendezvous location is agreed upon, not requiring any knowledge of the locations of other drifters. •

Figure 2 depicts the evolution of a group of 4 drifters executing the proposed coordination algorithm. Note that because the drifters start near the top/bottom of the ocean, their depth-control authority is saturated and some of them are therefore pushed in the wrong direction. As they move towards the middle, their depth control becomes eventually unsaturated and then they are able to rendezvous successfully.

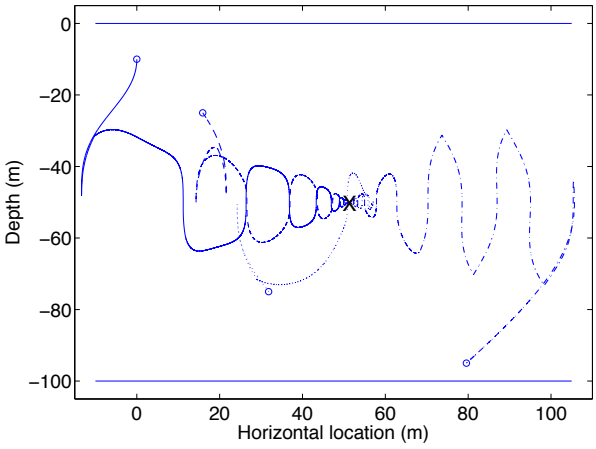

Fig. 2. This plot illustrates an evolution of 4 drifters with Lagrangian dynamics (9) executing the proposed distributed rendezvous algorithm (6) and (10). The parameters are $k = \frac{2\pi}{100}\frac{1}{\mathrm{m}}$, $\omega = \frac{2\pi}{1000}\frac{1}{\mathrm{s}}$, $\alpha = 10$, and $H = 100\mathrm{m}$. The drifters are initially at $(0, -10)$, $(16, -25)$, $(32, -75)$ and $(80, -95)$, marked by 'o's. Their neighbors are the drifters initially on either side of them. The network converges to a point around $(52, -50)$, marked by 'x'.

Remark 4.6 (Time-varying wave parameters and unmodeled dynamics) Although the chosen wave model is qualitatively realistic to true internal waves, they rarely correspond perfectly to the model, perhaps due to coupling with other physical ocean processes. For general slowly time-varying wave parameters, and with online estimation of these parameters by the drifters, the proposed coordination algorithm would still achieve convergence of the group to a neighborhood of each other. In the case where one can model the wave with piecewise-constant parameters, drifters could switch control laws as the wave parameters change. The robustness analysis of the forthcoming section also speaks to the fact that sufficiently small unmodeled dynamics do not destroy the algorithm convergence properties. •

4.3 Robustness against errors and unmodeled dynamics

Here we investigate the robustness of the proposed coordination strategy for rendezvous against several sources of error. We start by considering the presence of additive error in the virtual control law (7),

$$\dot{x}_i = -A\frac{\alpha\pi}{H}\tanh(Lx)_i \sin^2(kx_i - \omega t + \phi) + \gamma_i, \quad (12)$$

for $i \in \{1, \dots, N\}$. Here, the error γ_i may be an arbitrary function of errors in state or parameter estimation.

Proposition 4.7 (Robustness against additive error) *Given any $T > 0$ and $K > 1$, consider the dynamics (12) and assume*

$$|\gamma_i| \le \bar{\gamma} < \min\Big(\frac{\omega}{k} - A\frac{\alpha\pi}{H}, \frac{A\frac{\alpha\pi}{H}S(T)\tanh\big((K-1)2|\mathcal{N}|_{\max}\frac{\omega}{k}T\big)(K-1)}{KTN(K+1)}\Big),$$

for $i \in \{1, \dots, N\}$, where

$$S(T) = \min_{\{\Phi:[0,T]\to\mathbb{R} \mid \dot{\Phi}_i \in I\}} \int_0^T \sin^2(\Phi(\tau))d\tau$$

and the interval $I = [-\omega - k(A\frac{\alpha\pi}{H} + \bar{\gamma}), -\omega + k(A\frac{\alpha\pi}{H} + \bar{\gamma})]$. For $\bar{\gamma}$ sufficiently small, there exists $d(\bar{\gamma}(T))$ such that, in finite time, the distance between any two drifters remains at most $d(\bar{\gamma}(T))$. Conversely, for d arbitrarily small, there exists $\bar{\gamma}_*(T) > 0$ such that $d(\bar{\gamma}(T)) \le d$ for all $\bar{\gamma} \le \bar{\gamma}_*(T)$.

PROOF. We begin by explicitly characterizing, in terms of the function $V(x) = \frac{1}{2}x^T Lx$, a region where we can lower bound the decrease of V by a constant over a time interval of a given arbitrary length $T > 0$. Once this is established, we employ this fact to show the result. Using (8), we obtain

$$V(x(t+T)) - V(x(t)) = \int_t^{t+T} \sum_{i=1}^{N} (Lx(\tau))_i \cdot$$
$$\cdot\left(-A\frac{\alpha\pi}{H}\tanh(Lx(\tau))_i \sin^2(kx_i(\tau) - \omega\tau + \phi) + \gamma_i(\tau)\right)d\tau.$$

Using the minimum and maximum values that terms take over the period T, this can be upper bounded as

$$V(x(t+T)) - V(x(t)) \leq \sum_{i=1}^{N} \max_{\xi\in[t,t+T]} |Lx(\xi)_i|\bar{\gamma}T - A\frac{\alpha\pi}{H}\sum_{i=1}^{N} \min_{\xi\in[t,t+T]} (Lx(\xi))_i \tanh(Lx(\xi))_i \cdot \cdot \int_t^{t+T} \sin^2(kx_i(\tau) - \omega\tau + \phi)d\tau. \quad (13)$$

From (12), note that $|\dot{x}_i| \leq A\frac{\alpha\pi}{H} + \bar{\gamma}$, which together with the hypothesis $\bar{\gamma} < \frac{\omega}{k} - A\frac{\alpha\pi}{H}$ implies that $\Phi_i(t) = kx_i(t) - \omega t + \phi$ is strictly decreasing and its derivative is bounded, belonging to the interval $I = [-\omega - k(A\frac{\alpha\pi}{H} + \bar{\gamma}), -\omega + k(A\frac{\alpha\pi}{H} + \bar{\gamma})]$. As a consequence, we deduce

$$S(T) = \min_{\{\Phi:[0,T]\to\mathbb{R} \mid \dot{\Phi}_i\in I\}} \int_0^T \sin^2(\Phi(\tau))d\tau,$$

is strictly positive. Substituting into (13), we obtain

$$V(x(t+T)) - V(x(t)) \leq \Big(\sum_{i=1}^{N} \max_{\xi\in[t,t+T]} |Lx(\xi)_i|\bar{\gamma}T - A\frac{\alpha\pi}{H}S(T)\sum_{j=1}^{N} \min_{\xi\in[t,t+T]} (Lx(\xi))_j \tanh(Lx(\xi))_j\Big).$$

Since the drifters' velocities are bounded as $|\dot{x}_i| \leq \frac{\omega}{k}$,

$$V(x(t+T))-V(x(t)) \leq \bar{\gamma}TN\Big(\|Lx(t)\|_\infty + 2|\mathcal{N}|_{\max}\frac{\omega}{k}T\Big) - A\frac{\alpha\pi}{H}S(T)\tanh\big(\|Lx(t)\|_\infty - 2|\mathcal{N}|_{\max}\frac{\omega}{k}T\big)\cdot \cdot (\|Lx(t)\|_\infty - 2|\mathcal{N}|_{\max}\frac{\omega}{k}T),$$

if $\|Lx(t)\|_\infty > 2|\mathcal{N}|_{\max}\frac{\omega}{k}T$. Our strategy now is to grow this set by a multiplicative factor K. As a function of K, we find an upper bound on the error $\bar{\gamma}_{\max}(K)$ for which the V decreases by a strictly positive constant over the period T. We choose a gain $K > 1$, let

$$\bar{\gamma}_{\max}(K) = \frac{A\frac{\alpha\pi}{H}S(T)\tanh\big((K-1)2|\mathcal{N}|_{\max}\frac{\omega}{k}T\big)(K-1)}{KTN(K+1)}. \quad (14)$$

Then, if $\bar{\gamma} \leq \bar{\gamma}_{\max}(K)$,

$$V(x(t+T))-V(x(t)) \leq A\frac{\alpha\pi}{H}S(T)(\|Lx(t)\|_\infty - 2|\mathcal{N}|_{\max}\frac{\omega}{k}T)\cdot \cdot \tanh\big(\|Lx(t)\|_\infty - 2|\mathcal{N}|_{\max}\frac{\omega}{k}T\big) \Bigg(\frac{1}{K}\Big(\frac{\tanh\big((K-1)2|\mathcal{N}|_{\max}\frac{\omega}{k}T\big)}{\tanh\big(\|Lx(t)\|_\infty - 2|\mathcal{N}|_{\max}\frac{\omega}{k}T\big)}\Big) \Big(\frac{\|Lx(t)\|_\infty + 2|\mathcal{N}|_{\max}\frac{\omega}{k}T}{\|Lx(t)\|_\infty - 2|\mathcal{N}|_{\max}\frac{\omega}{k}T}\Big)\Big(\frac{K-1}{K+1}\Big) - 1\Bigg), \quad (15)$$

for $\|Lx(t)\|_\infty \geq 2|\mathcal{N}|_{\max}\frac{\omega}{k}T$. By growing the set by gain K to $\|Lx(t)\|_\infty \geq 2|\mathcal{N}|_{\max}K\frac{\omega}{k}T$, we have that

$$\frac{\tanh\big((K-1)2|\mathcal{N}|_{\max}\frac{\omega}{k}T\big)}{\tanh\big(\|Lx(t)\|_\infty - 2|\mathcal{N}|_{\max}\frac{\omega}{k}T\big)} \leq 1, \qquad \frac{\|Lx(t)\|_\infty + 2|\mathcal{N}|_{\max}\frac{\omega}{k}T}{\|Lx(t)\|_\infty - 2|\mathcal{N}|_{\max}\frac{\omega}{k}T} \leq \frac{K+1}{K-1}$$

for all $\|Lx(t)\|_\infty \geq 2|\mathcal{N}|_{\max}K\frac{\omega}{k}T$. Using these inequalities to simplify (15), we obtain

$$V(x(t+T)) - V(x(t)) \leq A\frac{\alpha\pi}{H}S(T)\tanh\big(\|Lx(t)\|_\infty - 2|\mathcal{N}|_{\max}\frac{\omega}{k}T\big) (\|Lx(t)\|_\infty - 2|\mathcal{N}|_{\max}\frac{\omega}{k}T)\Big(\frac{1}{K} - 1\Big) \leq -C_0 < 0,$$

when $\|Lx(t)\|_\infty \geq 2|\mathcal{N}|_{\max}K\frac{\omega}{k}T$, where

$$C_0 = A\frac{\alpha\pi}{H}S(T)\tanh\big((K-1)2|\mathcal{N}|_{\max}\frac{\omega}{k}T\big)\cdot \cdot ((K-1)^2 2|\mathcal{N}|_{\max}\frac{\omega}{kK}T).$$

From (1), $\|Lx\|_\infty^2 \geq \frac{1}{N}\|Lx\|_2^2 \geq \frac{2\lambda_2(L)}{N}V(x)$, we deduce that if $V(x(t)) \geq \frac{2N}{\lambda_2(L)}(|\mathcal{N}|_{\max}K\frac{\omega}{k}T)^2$, then $V(t+T) - V(t) \leq -C_0$. As a consequence, for any initial $V(x(0))$, we deduce that the set $V(x) \leq \frac{2N}{\lambda_2(L)}(|\mathcal{N}|_{\max}K\frac{\omega}{k}T)^2$ is reached in finite time. Once this happens, if there is a time t when $V(x(t)) = \frac{2N}{\lambda_2(L)}(|\mathcal{N}|_{\max}K\frac{\omega}{k}T)^2$, after T seconds one has again $V(x(t+T)) \leq \frac{2N}{\lambda_2(L)}(|\mathcal{N}|_{\max}K\frac{\omega}{k}T)^2$. Furthermore, because

$$\mathcal{L}_{(12)}V(x(t)) = x^T Lv \leq \|Lx\|_2\frac{\omega}{k} \leq \sqrt{2\lambda_N(L)}\frac{\omega}{k}\sqrt{V(x(t))},$$

we can upper bound $V(x(t+T))$ by

$$V(x(t+T)) \leq \Big(\frac{\sqrt{2\lambda_N(L)}\frac{\omega}{k}}{2}T + V(t)^{\frac{1}{2}}\Big)^2.$$

Using this upper bound, we conclude that once the set $V(x) \leq \frac{2N}{\lambda_2(L)}(|\mathcal{N}|_{\max}K\frac{\omega}{k}T)^2$ is reached, the trajectory

never leaves the set

$$V(x) \leq \left(\frac{\sqrt{2}\omega}{k} T \Big(\frac{\sqrt{\lambda_N(L)}}{2} + \sqrt{\frac{N}{\lambda_2(L)}} |\mathcal{N}|_{\max} K \Big) \right)^2. \tag{16}$$

The first result in the statement now follows by noting that an upper bound on V directly translates into an upper bound on the distance between any two drifters because

$$V(x) = \frac{1}{2} x^T L x = \frac{1}{4} \sum_{i=1}^{N} \sum_{j=1}^{N} a_{i,j} (x_i - x_j)^2,$$

where $a_{i,j} = 1$ if there exists an edge from i to j and $a_{i,j} = 0$ otherwise. In the worst case, $x_{\max} - x_{\min} \leq 2\sqrt{V(x)}$. The second result follows from first noting a desired bound d implies an upper bound on K and T to satisfy (16). These bounds provide an upper bound for $\bar{\gamma}_{\max}$ through (14). □

The bound in Proposition 4.7 enforces that (i) the perturbation is never large enough to make the drifter move faster than the wave (which is physically impossible) and (ii) over an interval of length T, the Lyapunov function decreases when the drifters are sufficiently far from agreement. Figure 3 depicts an evolution of the first-order virtual rendezvous dynamics with additive error (12). Here one can see that the drifters converge to a neighborhood around rendezvous. Note that there is a net horizontal displacement in the wave propagation direction caused by the internal wave. This is due to the drifters never quite converging to a depth of $\frac{H}{2}$, where there is no horizontal motion.

To finish this section, we consider the true drifter dynamics (3) for each $i \in \{1, \ldots, N\}$ subject to both additive errors

$$\dot{x}_i = \frac{\alpha\pi}{H} \cos\left(\frac{\pi z_i}{H}\right) \sin(k x_i - \omega t + \phi) + \gamma_i, \tag{17}$$

$\dot{z}_i = u_i$, and actuation errors of the form

$$u_i(d, x, t) = \tag{18}$$
$$\operatorname{sat}_M \big(\frac{H}{\pi\sqrt{1 - d_i^2}} (C \operatorname{sgn}(d_i - w_i(x,t)) - \dot{w}_i(x,t)) + \delta_i \big).$$

Interestingly, it is clear from this expression that if the actuation error is small enough, the term arising from the discontinuous function sgn in the controller cancels the effect of the disturbance, making the algorithm inherently robust. We formalize this next.

Lemma 4.8 (Robustness to actuation error) *Assume $\delta_i \leq \bar{\delta} < H\epsilon h(A)/\pi\sqrt{1 - d_i(0)^2}$, for all $i \in \{1, \ldots, N\}$. Then, for any $x(0) \in \mathbb{R}^N$, $z(0) \in (0, H)^N$, and $M \in \mathbb{R}_{>0}$, the error variable e_i evolving under the closed-loop system (17) with (6) and (18) converges to 0 in finite time.*

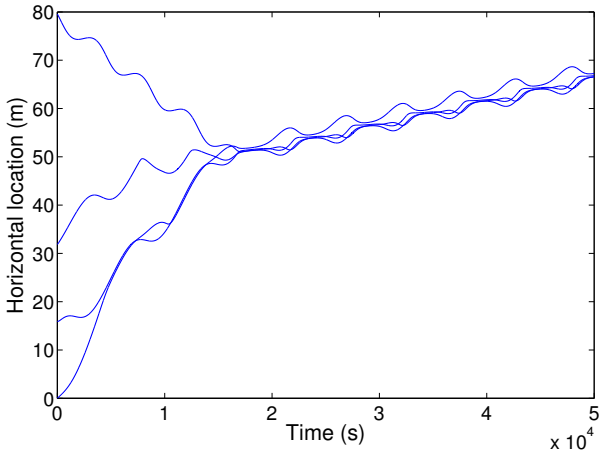

Fig. 3. This plot illustrates an evolution of the virtual rendezvous dynamics with additive error (12) for a group of 4 drifters. The parameters are $k = \frac{2\pi}{100}\frac{1}{\text{m}}$, $\omega = \frac{2\pi}{1000}\frac{1}{\text{s}}$, $\alpha = 10$, and $H = 100$m. The drifters are initially at 0, 16, 32 and 80 meters. Each drifter has a constant error of .02, −.005, −.01, and .005, respectively. They converge to a neighborhood around each other of about 5 meters. Note the net horizontal displacement in the wave propagation direction.

As a consequence of this result, in finite time, the dynamics (17) becomes exactly (12), and therefore the robustness properties asserted in Proposition 4.7 hold too. This also implies that, in the absence of additive errors, if the assumptions of Theorem 4.4 are met, the drifters asymptotically rendezvous despite the actuation errors.

5 Rendezvous of second-order drifters

In this section we adapt the method developed in Section 4 to the linear, second-order model (4) for the drifter dynamics. As we did before, our starting point is the assumption that all drifters know the wave parameters (in fact, one can determine them using measurements collected by the drifters and fitting them to the dynamics (4) induced by the internal wave but, for reasons of space, we do not present this discussion here).

5.1 Virtual rendezvous control law

We begin by designing a control law w_i, $i \in \{1, \ldots, N\}$, assuming that the drifters can directly actuate their own x-acceleration through their depth, i.e.,

$$\dot{x}_i = v_i, \quad \dot{v}_i = -\frac{c_d}{m}(v_i - \frac{\alpha\pi}{H} w_i \sin(k x_i - \omega t + \phi)),$$

Our proposed distributed design is

$$w_i(x, v, t) = -A \sin(k x_i - \omega t + \phi) \tanh(L(\frac{c_d}{m} x + v)_i) \tag{19}$$

so that the closed-loop dynamics takes the form

$$\dot{x}_i = v_i, \tag{20a}$$
$$\dot{v}_i = -\frac{c_d}{m}\big(v_i + \frac{\alpha\pi}{H}\sin^2(kx_i - \omega t + \phi)\cdot A\tanh(L(\frac{c_d}{m}x + v)_i\big). \tag{20b}$$

The next result shows that each drifters' sum of position and velocity remains bounded.

Lemma 5.1 (Boundedness of the sum of position and velocity) *Given any initial condition $(x(0), v(0)) \in \mathbb{R}^{2N}$ for the group of drifters, the network trajectory under (20) satisfies $\frac{c_d}{m}x(t) + v(t) \in [(\frac{c_d}{m}x(0) + v(0))_{\min}, (\frac{c_d}{m}x(0) + v(0))_{\max}]^N$ for all $t \geq 0$.*

The proof of this result uses the same argument employed in Lemma 4.1.

Building on Lemma 5.1, we next show that, in fact, the position of the drifters remains bounded as well.

Lemma 5.2 (Boundedness of position) *Given any initial condition $(x(0), v(0)) \in \mathbb{R}^{2N}$ for the group of drifters, the network trajectory under (20) satisfies $x(t) \in [x(0)_{\min}, x(0)_{\max}]^N$, for all $t \geq 0$.*

PROOF. From Lemma 5.1, we have $\frac{c_d}{m}x(t) + v(t) \in [(\frac{c_d}{m}x(0) + v(0))_{\min}, (\frac{c_d}{m}x(0) + v(0))_{\max}]^N$ for all $t \geq 0$. This implies that, if drifter $i \in \{1, \dots, N\}$ has $\frac{c_d}{m}x_i(0) > (\frac{c_d}{m}x(0)+v(0))_{\max}$ (resp. $\frac{c_d}{m}x_i(0) < (\frac{c_d}{m}x(0)+v(0))_{\min}$), then $\dot{x}_i(0) < 0$ (resp. $\dot{x}_i(0) > 0$), which shows the result. □

We are now ready to show that the drifters all converge to rendezvous in the x-direction under the control law (20).

Proposition 5.3 (Asymptotic network rendezvous) *Given any initial condition $(x(0), v(0)) \in \mathbb{R}^{2N}$ for the group of drifters, the dynamics (20) makes the network rendezvous in the x-direction: for all i, j in $\{1, \dots, N\}$*

$$\lim_{t\to\infty} x_i(t) - x_j(t) = 0, \qquad \lim_{t\to\infty} v_i(t) = 0.$$

PROOF. Consider the disagreement function $V(x, v) = \frac{1}{2}(\frac{c_d}{m}x + v)^T L(\frac{c_d}{m}x + v)$, whose Lie derivative is

$$\mathcal{L}_{(20)}V(x,v) = \sum_{i=1}^{N}(L(\frac{c_d}{m}x + v))_i \frac{c_d}{m}\frac{\alpha\pi}{H}\cdot \sin^2(kx_i - \omega t + \phi)A\tanh(L(\frac{c_d}{m}x + v)_i) \leq 0. \tag{21}$$

Since V is non-increasing and lower-bounded by 0, $V(x(t), v(t))$ converges as $t \to \infty$. Therefore,

$$\lim_{t\to\infty} V(x(t), v(t)) - V(x(0), v(0)) = \lim_{t\to\infty}\int_0^t \mathcal{L}_{(20)}V(x(s), v(s))ds$$

exists and is finite. Furthermore, because x and v remain bounded by Lemmas 5.1 and 5.2, $\frac{d}{dt}\mathcal{L}_{(20)}V(x(t), v(t))$ is bounded for all t, which implies that $\mathcal{L}_{(20)}V(x(t), v(t))$ is uniformly continuous on $\mathbb{R}_{\geq 0}$. Therefore, the application of Lemma 2.1 to $\mathcal{L}_{(20)}V(x(t), v(t))$ yields $\lim_{t\to\infty}\mathcal{L}_{(20)}V(x(t)) = 0$. Since each summand of $\mathcal{L}_{(20)}V(x(t))$ is non-positive, in the limit, all summands must converge to zero. Considering the first summand, we suppose that $\lim_{t\to\infty}\sin^2(kx_1 - \omega t + \phi) = 0$ and show a contradiction. This condition implies that $kx_1 - \omega t + \phi$ converges to the discrete set $\{\dots, -2\pi, -\pi, 0, \pi, 2\pi, \dots\}$. However, convergence to a discrete set implies convergence to one of its points, which, in turn, implies that x_1 diverges, contradicting Lemma 5.2. Reasoning in a similar way, one deduces $L(\frac{c_d}{m}x(t) + v(t))$ converges to zero. Note that for any $i \in \{1, \dots, N\}$, the derivative of $\frac{c_d}{m}x_i + v_i$ is

$$\frac{c_d}{m}v_i + \dot{v}_i = -\frac{c_d}{m}\frac{\alpha\pi}{H}\sin^2(kx_i - \omega t + \phi)\cdot A\tanh(L(\frac{c_d}{m}x + v))_i,$$

which we now know converges to zero. This, in turn, implies that v_i converges to zero, for all $i \in \{1, \dots, N\}$. Thus, we conclude that $L(x(t))$ converges to 0, or, in other words, all drifters agree on their $x-$variables. □

5.2 Backstepping depth-control law

As before, we re-define the control authority u_i to be the remaining control after canceling the vertical dynamics, so that the dynamics looks,

$$\dot{x}_i = v_i,$$
$$\dot{v}_i = -\frac{c_d}{m}(v_i - \frac{\alpha\pi}{H}\cos(\frac{\pi z_i}{H})\sin(kx - \omega t + \phi)),$$
$$\dot{z}_i = u_i.$$

Then, going through the same variable changes as for the Lagrangian case, we arrive at

$$\dot{x}_i = v_i \tag{22a}$$
$$\dot{v}_i = -\frac{c_d}{m}(v_i - \frac{\alpha\pi}{H}w_i\sin(kx_i - \omega t + \phi)) + \frac{c_d}{m}\frac{\alpha\pi}{H}\sin(kx_i - \omega t + \phi)e_i, \tag{22b}$$
$$\dot{e}_i = -\frac{\pi}{H}\sqrt{1 - d_i^2}u_i - \dot{w}_i. \tag{22c}$$

We select the depth-control law with the same structure as (10) but now with the virtual control law given by (19). The next result characterizes the asymptotic convergence properties of the closed-loop system.

Theorem 5.4 (Asymptotic network rendezvous) *For any initial position $(x(0), v(0)) \in \mathbb{R}^{2N}$, depth $z(0) \in (0, H)^N$, $\epsilon \in \mathbb{R}_{>0}$, and bound $M \in \mathbb{R}_{>0}$ on the magnitude of depth control actuation, let the magnitude A of the control law* (19) *satisfy*

$$\frac{\big(A^2\alpha\pi(2|\mathcal{N}|_{\max}\frac{c_d}{m}+k)+\omega AH\big)(1+\epsilon)}{\pi(1-(1+\epsilon)^2A^2)} \leq M,$$

and the gain $C \geq (\frac{\alpha\pi}{H}A^2(2|\mathcal{N}|_{\max}\frac{c_d}{m}+k)+\omega A)(1+\epsilon)$ in the depth-control law (10)*. Then, all drifters asymptotically rendezvous under the dynamics of* (22) *with the controllers* (19) *and* (10)*, i.e., for all $i, j \in \{1, \dots, N\}$,*

$$\lim_{t\to\infty} x_i(t) - x_j(t) = 0, \quad \lim_{t\to\infty} v_i(t) = 0, \quad \lim_{t\to\infty} z_i(t) = \frac{-H}{2}.$$

PROOF. Under the stated hypotheses, note that, for each $i \in \{1, \dots, N\}$, we have $|w_i| \leq A$ and $|\dot{w}_i| \leq (\frac{\alpha\pi}{H}A^2(2|\mathcal{N}|_{\max}\frac{c_d}{m}+k)+\omega A) = h(A)$. Then, Lemma 4.3 implies that the depth-control law converges to the virtual rendezvous control law in finite time. After this, Proposition 5.3 guarantees asymptotic rendezvous in the wave propagation direction. Depth convergence follows by noting that, in finite time, $d_i(t) = w_i(t)$ and $w_i(t)$ converges to 0. □

Figure 4 depicts the evolution of 5 drifters with second-order dynamics executing the coordination algorithm. Note that even though drifters start near the internal wave mean depth, where their depth-control authority is unsaturated, the flow pushes some of them in the wrong direction. These drifters then change depth until the flow is aligned with their desired direction of motion. By repeatedly switching between being above and below the wave depending on the flow direction, the drifters asymptotically rendezvous.

One can also study the algorithm robustness properties along lines similar to those of the first-order case.

For instance, in the case of additive errors in the virtual controller,

$$\dot{x}_i = v_i + \gamma_{x,i}, \tag{23a}$$
$$\dot{v}_i = -\frac{c_d}{m}(v_i - \frac{\alpha\pi}{H}w_i \sin(kx_i - \omega t + \phi)) + \gamma_{v,i}, \tag{23b}$$

one can readily adapt Proposition 4.7 to show that under (23), the drifters converge to a neighborhood around agreement in $\frac{c_d}{m}x + v$. Figure 5 illustrates this result. The algorithm robustness against actuation errors in the depth-controller can also be stated in a similar result to Lemma 4.8 by just appropriately changing the function h in its statement.

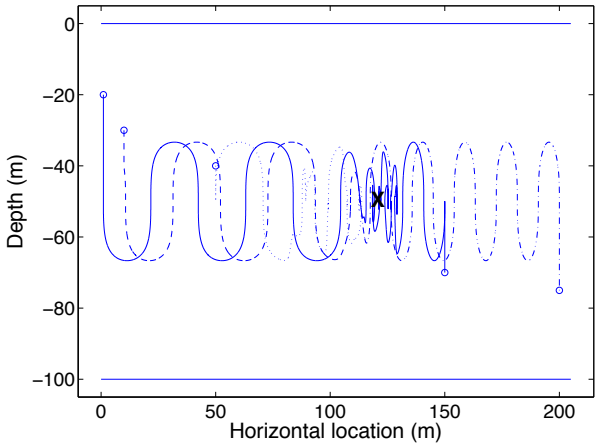

Fig. 4. This plot illustrates an evolution of 5 drifters with second-order dynamics (4) executing the proposed distributed rendezvous algorithm (19)-(10). The parameters are $k = \frac{2\pi}{100}\frac{1}{\text{m}}$, $\omega = \frac{2\pi}{1000}\frac{1}{\text{s}}$, $\alpha = 10$, $\frac{c_d}{m} = 4$, and $H = 100$m. The drifters are initially located at $(1, -20)$, $(10, -30)$, $(50, -40)$, $(150, -70)$ and $(200, -75)$ with no horizontal velocity, marked by 'o's. Their neighbors are the drifters initially on either side of them. The network converges to a point around $(113, -50)$, marked by 'x'.

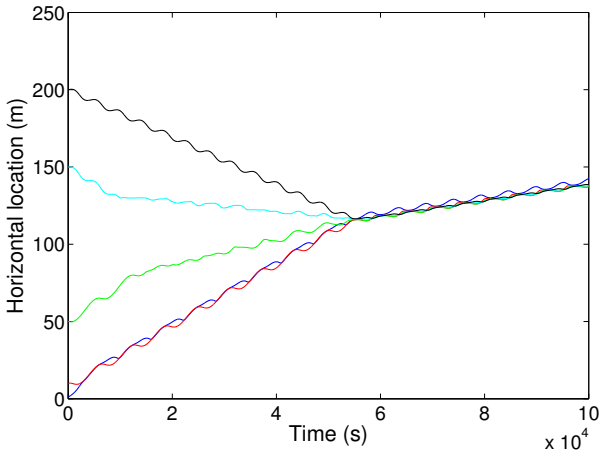

Fig. 5. This plot illustrates an evolution of the virtual rendezvous dynamics with additive error (23). The parameters are $k = \frac{2\pi}{100}\frac{1}{\text{m}}$, $\omega = \frac{2\pi}{1000}\frac{1}{\text{s}}$, $\alpha = 10$, $\frac{c_d}{m} = 4$, and $H = 100$m. The drifters are initially located at 1, 10, 50, 150 and 200 meters with no horizontal velocity. They have constant errors in (position, velocity) of $(.002, .08)$, $(-.004, -.02)$, $(.004, -.04)$, $(-.004, .02)$, and $(.002, .02)$ in (meters, meters per second). They converge to a neighborhood around each other of about 5 meters. Note that there is a net horizontal displacement in the wave propagation direction. This is due to the drifters never quite converging to a depth of $\frac{H}{2}$, where there is no horizontal motion.

Remark 5.5 (Extension to individual drifter location control) We note that the presented algorithm can be extended to allow the drifters to converge to an arbitrary horizontal location. For a given desired location ξ, drifter i can reach it by moving towards a static

'virtual' drifter located at ξ. As a result, drifter i will asymptotically converge to the horizontal location ξ and depth $\frac{-H}{2}$. •

6 Conclusions

We have considered a group of depth-actuated robotic drifters deployed in a ocean flowfield generated by an internal wave that seek to perform coordinated rendezvous for easy retrieval. We have synthesized a distributed algorithmic solution that allows them to rely on the ocean flowfield to asymptotically rendezvous in the wave propagation direction for two different (Lagrangian and drag-based) dynamical drifter models. Our design has employed a backstepping methodology, where we first synthesize a rendezvousing controller assuming direct control in the horizontal direction is available and then design a depth-control law that is guaranteed to converge to this controller in finite time. We have also investigated the algorithms' robustness properties of the depth-control law against actuation errors and the virtual control law against errors in the knowledge of the flowfield or the state of other drifters. Future work will be devoted to extend our results to increasingly realistic scenarios, including an internal wave plus nonperiodic currents, the consideration of nonlinear second-order drifter dynamics where the drag force is proportional to the square of the relative velocity, the synthesis of strategies that only rely on relative distance inter-drifter measurements, and scenarios where the drifters' control authority cannot always completely cancel the vertical wave dynamics.

Acknowledgments

The authors would like to thank Professor Peter Franks at the Scripps Institute of Oceanography for multiple discussions and for referring us to [Thorpe, 1968]. This research was supported by NSF award OCE-0941692.

References

F. Bullo, J. Cortés, and S. Martínez. *Distributed Control of Robotic Networks*. Applied Mathematics Series. Princeton University Press, 2009. ISBN 978-0-691-14195-4. Electronically available at `http://coordinationbook.info`.

F. Cazenave. Internal waves over the continental shelf in South Monterey Bay. Master's thesis, San Jose State University, San Jose, CA, USA, 2008.

L. DeVries and D. Paley. Multi-vehicle control in a strong flowfield with application to hurricane sampling. *AIAA Journal of Guidance, Control, and Dynamics*, 35(3):794–806, 2012.

P. Franks. Spatial patterns in dense algal blooms. *Limnology and Oceanography*, 42(5):1297–1305, 1997.

H. J. Freeland and P. F. Cummins. Argo: A new tool for environmental monitoring and assessment of the world's oceans, and example from the N.E. Pacific. *Progress in Oceanography*, 64 (1):31–44, 2005.

R. Graham and J. Cortés. Adaptive information collection by robotic sensor networks for spatial estimation. *IEEE Transactions on Automatic Control*, 57(6):1404–1419, 2012.

S. Hamdi, B. Morse, B. Halphen, and W. Scheisser. Analytical solutions of long nonlinear internal waves: Part I. *Natural Hazards*, 57(3):597–607, 2011.

Y. Han, R. A. de Callafon, J. Cortés, and J. Jaffe. Dynamic modeling and pneumatic switching control of a submersible drogue. In *International Conference on Informatics in Control, Automation and Robotics*, volume 2, pages 89–97, Funchal, Madeira, Portugal, June 2010.

Jaffe Laboratory for Underwater Imaging. Autonomous Underwater Explorer project. . Scripps Institute of Oceanography, 2014. La Jolla, CA. http://jaffeweb.ucsd.edu.

J. Jouffroy, Q. Y. Zhou, and O. Zielinski. On active current selection for Lagrangian profilers. *Modeling, Identification, and Control*, 34(1):1–10, 2013.

H. K. Khalil. *Nonlinear Systems*. Prentice Hall, 3 edition, 2002. ISBN 0130673897.

A. Kwok and S. Martínez. Coverage maximization with autonomous agents in fast flow environments. *Journal of Optimization Theory & Applications*, 155(2):986–1007, 2012.

C. Lennert-Cody and P. Franks. Plankton patchiness in high-frequency internal waves. *Marine Ecology Progress Series*, 18: 59–66, 1999.

N. E. Leonard, D. Paley, F. Lekien, R. Sepulchre, D. M. Fratantoni, and R. Davis. Collective motion, sensor networks, and ocean sampling. *Proceedings of the IEEE*, 95(1):48–74, 2007. Special Issue on Networked Control Systems.

C. Nowzari and J. Cortés. Zeno-free, distributed event-triggered communication and control for multi-agent average consensus. In *American Control Conference*, pages 2148–2153, Portland, OR, 2014.

A. R. Osborne and T. L. Burch. Internal solitons in the Andaman Sea. *Science*, 208(4443):451–460, 1980.

M. Ouimet and J. Cortés. Coordinated rendezvous of underwater drifters in ocean internal waves. In *IEEE Conf. on Decision and Control*, pages 6099–6104, Los Angeles, CA, 2014a.

M. Ouimet and J. Cortés. Robust, distributed estimation of internal wave parameters via inter-drogue measurements. *IEEE Transactions on Control Systems Technology*, 22(3):980–994, 2014b.

D. Paley, F. Zhang, and N. Leonard. Cooperative control for ocean sampling: the glider coordinated control system. *IEEE Transactions on Control Systems Technology*, 16(4):735–744, 2008.

D. A. Paley and C. Peterson. Stabilization of collective motion in a time-invariant flowfield. *AIAA Journal of Guidance, Control, and Dynamics*, 32(3):771–779, 2009.

M. Perry and D. Rudnick. Observing the ocean with autonomous and Lagrangian platforms and sensors. *Oceanography*, 16(4): 31–36, 2003.

S. Petillo and H. Schmidt. Exploiting adaptive and collaborative AUV autonomy for detection and characterization of internal waves. *IEEE Journal of Oceanic Engineering*, 2013. To appear.

J. Pineda. Circulation and larval distribution in internal tidal bore warm fronts. *Limnology and Oceanography*, 44(6):1400–1414, 1999.

W. Ren and R. W. Beard. *Distributed Consensus in Multi-Vehicle Cooperative Control*. Communications and Control Engineering. Springer, 2008. ISBN 978-1-84800-014-8.

Y. Ru and S. Martínez. Coverage control in constant flow environments based on a mixed energy-time metric. *Automatica*, 49(9):2632–2640, 2013.

A. L. Shanks. Surface slicks associated with tidally forced internal waves may transport pelagic larvae of benthic invertebrates and fishes shoreward. *Marine Ecology Progress Series*, 13:311–315, 1983.

R. Susanto, L. Mitnik, and Q. Zheng. Ocean internal waves observed in the Lombok Strait. *Oceanography*, 18(4):80–87, 2005.

L. Techy, K. A. Morgansen, and C. A. Woolsey. Long-baseline ranging system for acoustic underwater localization of the seaglider underwater glider. Technical report, University of Washington, September 2010.

S. A. Thorpe. On the shape of progressive internal waves. *Trans-*

actions for the Royal Society of London. Series A, Mathematical and Phsyical Sciences, 263(1145):563–614, 1968.

J. R. Zeldis and J. B. Jillett. Aggregation of pelagic Mundia gregana (Fabncius) (Decapoda, Anomura) by coastal fronts and internal waves. *Journal of Plankton Research*, 4(4):839–857, 1982.

Y. Zhang, A. B. Baggeroer, and J. G. Bellingham. Spectral-feature classification of oceanographic processes using an autonomous underwater vehicle. *IEEE Journal of Oceanic Engineering*, 26(4):726–741, 2001.